

Journal of Materials Chemistry C

Accepted Manuscript



This is an *Accepted Manuscript*, which has been through the Royal Society of Chemistry peer review process and has been accepted for publication.

Accepted Manuscripts are published online shortly after acceptance, before technical editing, formatting and proof reading. Using this free service, authors can make their results available to the community, in citable form, before we publish the edited article. We will replace this *Accepted Manuscript* with the edited and formatted *Advance Article* as soon as it is available.

You can find more information about *Accepted Manuscripts* in the [Information for Authors](#).

Please note that technical editing may introduce minor changes to the text and/or graphics, which may alter content. The journal's standard [Terms & Conditions](#) and the [Ethical guidelines](#) still apply. In no event shall the Royal Society of Chemistry be held responsible for any errors or omissions in this *Accepted Manuscript* or any consequences arising from the use of any information it contains.

Amphotropic azobenzene derivatives with oligooxyethylene and glycerol based polar groups

Xiaoping Tan,^{‡a} Ruilin Zhang,^{‡ab} Chunxiang Guo,^a Xiaohong Cheng,^{*a} Hongfei Gao,^a Feng Liu,^{*c} Johanna R. Bruckner,^d Frank Giesselmann,^{*d} Marko Prehm,^e Carsten Tschierske^{*e}

[a] Key Laboratory of Medicinal Chemistry for Natural Resources, Chemistry Department, Yunnan University, Kunming, Yunnan 650091, P. R. China

Fax: (+86) 871 5032905

E-mail: xhcheng@ynu.edu.cn

[b] Forensic Medicine of Kunming Medical University, Kunming 650500, P. R. China

[c] State Key Laboratory for Mechanical Behavior of Materials, Xi'an Jiaotong University, Xi'an, 710049, P. R. China

Fax: (+86) 29 82663453

E-mail: feng.liu@mail.xjtu.edu.cn

[d] University of Stuttgart, Institute of Physical Chemistry, Pfaffenwaldring 55, D-075069, Stuttgart, Germany

Fax: (+49) 711-685-62569

E-mail: f.giesselmann@ipc.uni-stuttgart.de

[e] Institute of Chemistry, Organic Chemistry, Martin Luther University Halle-Wittenberg, Kurt-Mothes Str. 2, 06120 Halle/Saale, Germany

Fax: (+49) 345 55 27346

E-mail: carsten.tschierske@chemie.uni-halle.de

[‡]Both authors contributed equally to this work

Abstract: A series of amphiphilic azobenzenes with one to three lipophilic alkyl chains at one end and polar groups with oligooxyethylene (EO) and racemic 3-glycerol units at the opposite end was synthesized and their thermotropic and lyotropic liquid crystalline self-assemblies were studied by POM, DSC and XRD. Tilted and non-tilted lamellar phases with interdigitated double layer structure (SmC_d and SmA_d , respectively) were found for the compounds with a single alkyl chain, whereas hexagonal columnar phases were formed by the compounds with two or three alkyl chains. The effect of protic solvents, like formamide, ethylene glycol and water, was investigated for representative examples. For compounds with the single chain, induction and stabilization of SmA phases were observed, though broad regions of lyotropic SmC phases were retained in most cases. Depending on the structure of the polar group the hexagonal columnar phases were either removed or drastically stabilized by the solvents.

Photoisomerisation of the azobenzene chromophore was also studied in solution.

Keywords: amphotropic, azobenzene, lyotropic liquid crystal, thermotropic liquid crystal, self-assembly, photoisomerisation

1. Introduction

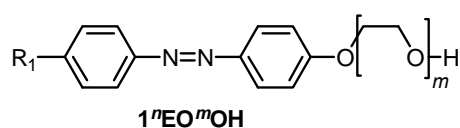
Design of molecules which can self-assemble into ordered nano-structures is of current interest for the general understanding of the processes of molecular self-assembly.^[1] Amphiphilic and anisometric compounds arose special interest as they can organize into ordered liquid crystalline (LC) superstructures with surprising complexity and great interest for material science as well as life science.^[2] By combining anisometric molecular shape and amphiphilic structure, both representing structural concepts supporting LC self-assembly, new amphotropic molecules can be obtained.^[3,4,5] Such molecules can display thermotropic and lyotropic LC phases and form well defined monolayers at interfaces.^[12] Typical examples are amphotropic LCs involving biphenyl,^[6,7,8] phenylpyrimidine^[9,10] and other rigid cores^[11,12] terminated with alky chain at one end and oligooxyethylene (EO) or glycerol-based groups at the other end.^[5] Amphotropic LC involving EO chains and glycerol units are potentially useful, for example, for design of nano-structured 1D, 2D or 3D ion conducting materials in combination with ionic liquids.^[13] On the other hand, LC azobenzene derivatives are attractive because of their photoresponsive properties caused by the *trans-cis* photoisomerization of the azobenzene units.^[14] Therefore, a wide diversity of azobenzene derivatived LC have been designed to introduce light-modulated functionalities, for example for application as organic light-driven actuators.^[15,16] Photoisomerizable amphiphiles can find applications in photoswitchable surfactants,^[17] for drug delivery,^[18] switchable vesicles^[19] and controlled gelation.^[20] Considering the vast variety of useful properties and potential applications, photoswitchable azobenzene based amphiphiles^[21,22,23,24,25,26,27] and especially photoswitchable amphotropic LC^[28,29,30] have received comparatively little attention to date. Herein we report the design, synthesis and thermotropic as well as lyotropic liquid crystalline self-assembly of new amphiphilic azobenzenes, consisting of EO^[31] or glycerol based polar groups or combinations of both involving one or two hydroxyl groups in the polar groups, and having one to three lipophilic *n*-alkyl chains at the opposite end.

In the notation of the compounds **1-3** (**1**^{*n*}EO^{*m*}OH to **3**^{*n*}EO^{*m*}OH and **1**^{*n*}EO^{*m*}(OH)₂ to **3**^{*n*}EO^{*m*}(OH)₂, see Scheme 1), the first number indicates the number of terminal *n*-alkyl chains and the superscript *n* gives the length of these chains. Note that in compounds of type **1** the single alkoxy chain is directly attached to the azobenzene core whereas for compounds of types **2** and **3** with more than only one alkoxy chains these chains are attached *via* an additional benzyloxy unit to the azobenzene core. EO indicates the presence of an EO chain with a number *m* of EO units in this chain. At the end OH denotes the presence of a single

CH₂Cl₂, Et₃N, 0 °C - 25 °C; *iii*) K₂CO₃, DMF, 90 °C, 12 h; *iv*) CH₃CN, K₂CO₃, 70 °C, 24 h; *v*) allyl bromide, NaH, THF, 70 °C, 12 h; *vi*) OsO₄, NMMNO, H₂O, acetone, 25 °C, 24 h.

2.2 Thermotropic self-assembly of the single chain compounds **1** in SmA and SmC phases

Table 1. Mesophases, transition temperatures ($T/^\circ\text{C}$) and transitional enthalpy values ($\Delta H/\text{kJ mol}^{-1}$) of the single chain compounds **1ⁿEO^mOH** with a single OH group. ^a



Comp	R ₁	m	Phase transitions ($T/^\circ\text{C}$)
1⁶EO³OH	C ₆ H ₁₃ O	3	Cr 102 [51.5] Iso
1⁶EO⁴OH	C ₆ H ₁₃ O	4	Cr 104 [49.5] Iso ^b
1¹²EO³OH	C ₁₂ H ₂₅ O	3	Cr 97 [35.6] SmC _d 106 [12.3] Iso
1¹²EO⁴OH	C ₁₂ H ₂₅ O	4	Cr 96 [42.6] SmC _d 113 [16.5] Iso
1¹⁸EO³OH	C ₁₈ H ₃₇ O	3	Cr 106 [52.1] SmC _d 114 [16.1] Iso

^a Transition temperature and enthalpy changes (in square brackets) were determined by DSC (peak temperature, first heating scan, 10 °C min⁻¹); abbreviations: Cr = crystalline solid; SmC_d = tilted smectic phase with double layer structure; Iso = isotropic liquid state. ^b supercooling was possible to 95 °C.

The phase transition temperatures and enthalpies of the azobenzene derivatives with a single alkyl chain (compounds **1**) are collected in Tables 1 and 2. No LC phases were found for the EO ethers with only one OH group and comparatively short hexyl chains (compounds **1⁶EO^mOH** with $m = 3,4$). Elongation of the alkyl chain leads to SmC phases. All compounds with terminal glycerol groups show smectic phases with enhanced stability compared to compounds with only a single OH group. Among them, compounds **1ⁿ(OH)₂** without EO units have enhanced mesophase stability compared to the related compounds **1ⁿEO^m(OH)₂** with additional EO units. SmC phases were found in all cases and for most compounds with glycerol groups, additional SmA phases are formed above the SmC phases. The SmA-SmC transitions have comparatively large enthalpy values ($\Delta H = 1.3\text{-}2.6 \text{ kJ mol}^{-1}$) for this kind of transition and thus this

phase transition appears to be first order. Fig. 1 shows representative DSC traces for compound $\mathbf{1}^{12}(\text{OH})_2$ with a SmC-SmA sequence. Interestingly, the Sm-Iso transition enthalpy values of the glycerol derivatives, having two terminal OH groups, are only about one half of those of the amphiphiles with only one hydroxyl group (compare Tables 1 and 2), which is discussed later.

Table 2. Mesophases, transition temperatures ($T/^\circ\text{C}$) and transitional enthalpy values ($\Delta H/\text{kJ mol}^{-1}$) of the single chain compounds $\mathbf{1}^n(\text{OH})_2$ and $\mathbf{1}^n\text{EO}^m(\text{OH})_2$ with a racemic 3-glyceryl group.^a

$\mathbf{1}^n\text{EO}^m(\text{OH})_2$

Comp	R ₁	m	Phase transitions ($T/^\circ\text{C}$)
$\mathbf{1}^{12}(\text{OH})_2$	C ₁₂ H ₂₅ O	0	Cr 156 [30.8] SmC _d 168 [1.3] SmA _d 176 [5.1] Iso
$\mathbf{1}^{14}(\text{OH})_2$	C ₁₄ H ₂₉ O	0	Cr 144 [31.1] SmC _d 166 [2.6] Iso
$\mathbf{1}^{12}\text{EO}^3(\text{OH})_2$	C ₁₂ H ₂₅ O	3	Cr 94 [18.6] SmC _d 129 [2.6] SmA _d 131 [6.0] Iso
$\mathbf{1}^{14}\text{EO}^3(\text{OH})_2$	C ₁₄ H ₂₉ O	3	Cr 95 [41.9] SmC _d 121 [2.0] SmA _d 126 [7.4] Iso

^a SmA_d = non-tilted smectic phase with double layer structure; for conditions and other abbreviations, see Table 1.

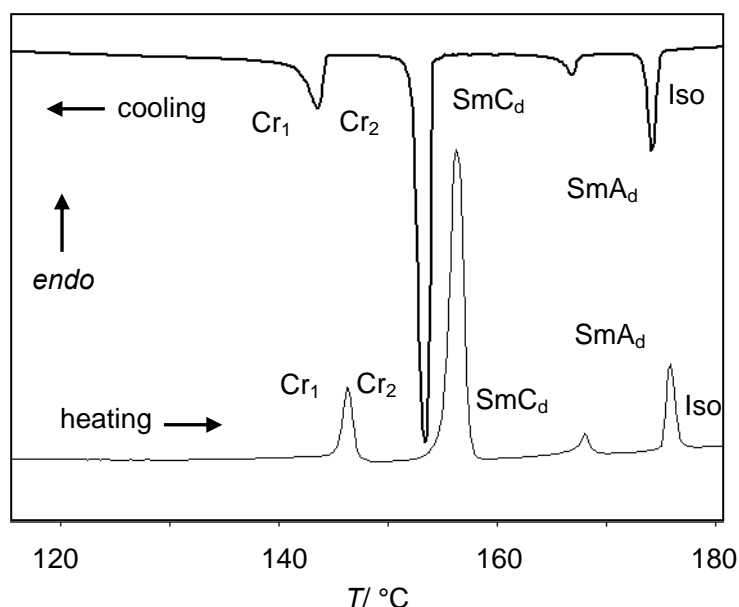


Figure 1. DSC traces of $\mathbf{1}^{12}(\text{OH})_2$ (10 K min⁻¹).

By microscopic investigation between non-treated glass plates through crossed polarizers, the smectic C phases of these compounds occur with typical broken fan and SmC schlieren textures^[34,35,36] (see Fig. 2a)

and the SmA phases are characterized by focal-conic fan-like textures and pseudoisotropic regions (Fig. 2b), often separated by oily streaks.

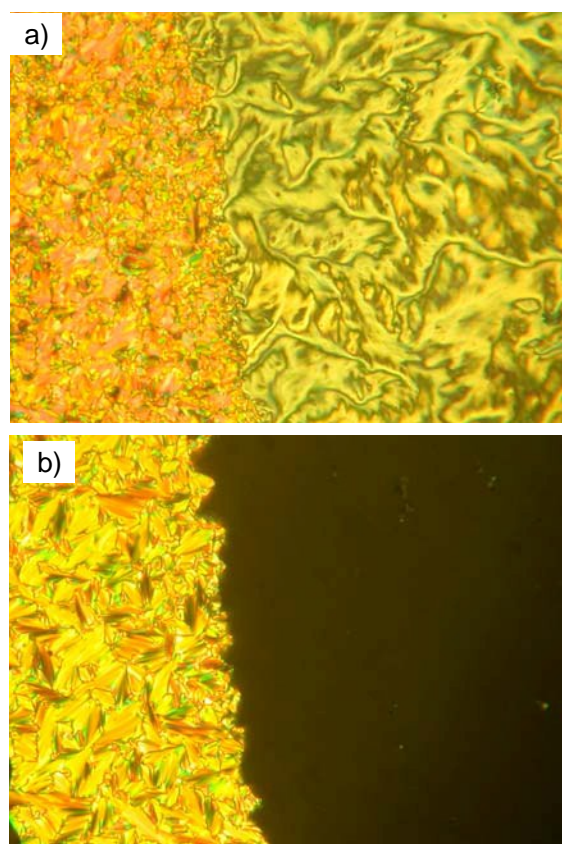


Figure 2. Textures of $1^{12}(\text{OH})_2$ in the a) SmC_d phase at $T = 167\text{ }^\circ\text{C}$ and b) in the SmA_d phase at $T = 169\text{ }^\circ\text{C}$ as observed on heating; at the right homeotropic alignment and at the left predominately planar alignment with fan texture.

Compounds $1^{12}\text{EO}^3\text{OH}$ and $1^{12}(\text{OH})_2$ were investigated as representative examples by X-ray diffraction (XRD; see Fig. 3). Diffuse wide angle scatterings with maxima at $d = 0.45\text{-}0.47\text{ nm}$, corresponding to the mean lateral distance between the molecules, indicate fluid smectic phases without in-plane order for all investigated compounds. This excludes the presence of other low temperature smectic mesophases^[37] and thus assignment to SmA and SmC was confirmed by XRD. The sharp fundamental and second-order pseudo-Bragg peaks in the small-angle regime originate from the long-range lamellar order along a single direction. For compound $1^{12}\text{EO}^3\text{OH}$ the layer reflection has a tilt angle $\theta = 29^\circ$ with respect to the maxima of the diffuse wide angle scattering, indicating the presence of a synclitic SmC phase with an average tilt of 29° (see Fig. 3c). The layer spacing is $d = 5.57\text{ nm}$ while the length of the molecule is only $L_{\text{max}} = 3.7\text{ nm}$ (calculated by MM2 method^[38] and assuming a molecule in the most stretched

conformation with *all-trans* conformation for the alkyl chains and EO chains^[39]). Thus the layer thickness is significantly larger than the molecular length ($d/L = 1.5$). Considering the tilt, the effective molecular length is reduced to $\cos 29^\circ L_{\text{mol}} = 3.24$ nm, leading to the effective d/L ratio of 1.72. This means that the layer distance is quite a bit smaller than twice the effective molecular length, indicating a bilayer structures with a partial intercalation of the alkyl chains as shown in Fig. 3d (SmC_d phase). The degree of alkyl chain intercalation could become smaller if there is strong disorder of the alkyl chains and especially of the EO chains.

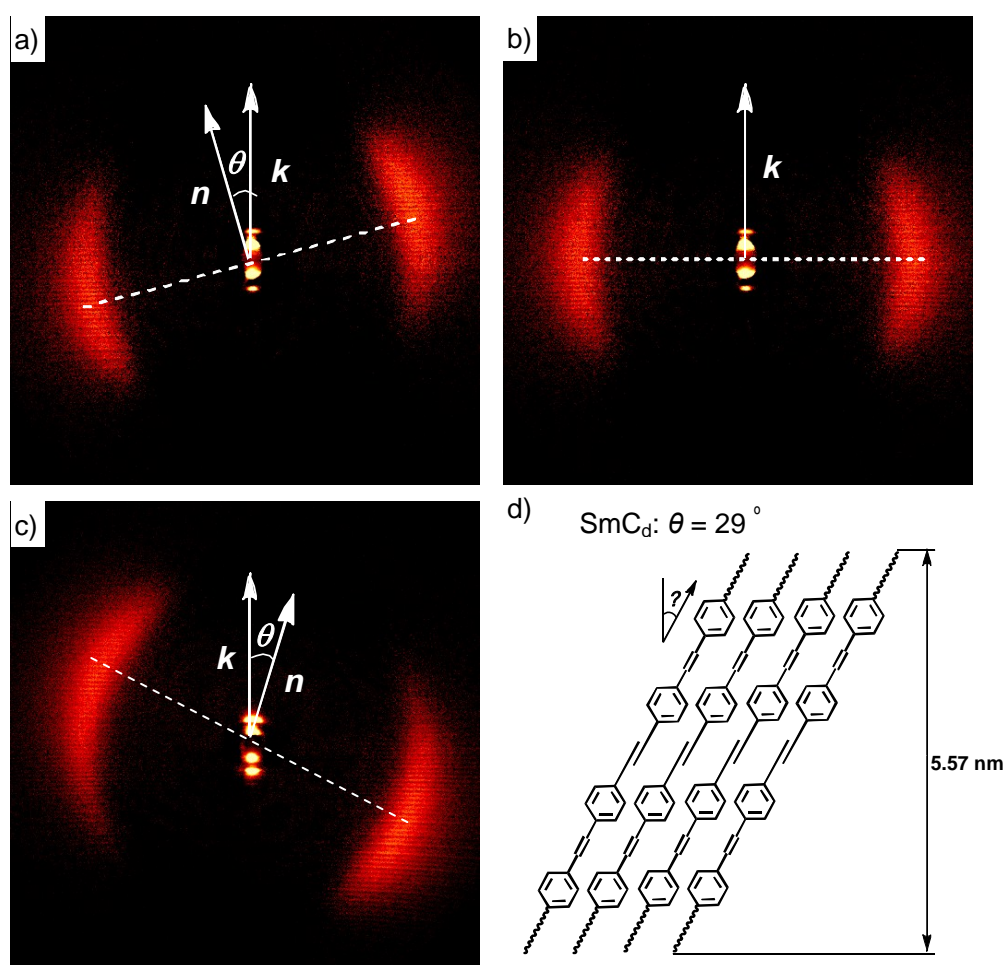


Figure 3. XRD patterns of the smectic phases after subtraction of the scattering in the isotropic liquid states: a) 2D-XRD pattern of a surface aligned sample of compound of $1^{12}(\text{OH})_2$ in the SmC_d phase at $T = 167$ °C and b) in the SmA_d phase at $T = 169$ °C and c) 2D pattern of a surface aligned sample of the SmC phase of $1^{12}\text{EO}^3\text{OH}$ at $T = 105$ °C; d) shows model of the molecular organization in one layer of the double layer SmC phase with partial intercalation of the alkyl chains; complete intercalation would lead to a $d \sim 5.2$ nm. For additional crystallographic data, see Tables S1- S3.

In the SmC phase of the glycerol derivative $1^{12}(\text{OH})_2$ with the same alkyl chain length, but without EO

units the thickness of the smectic layers is $d = 5.16$ nm at 167 °C and the tilt angle is only 12° (Fig. 3a). The layer thickness decreases to 5.05 nm at the transition from the SmA to the SmC phase at 167 °C, in line with the emerging uniform tilt angle of only 12° . The ratio $d/L = 1.56$ ($L_{\max} = 3.3$ nm) also indicates an intercalated bilayer structure for the SmC and SmA phases (SmC_d and SmA_d phases) with a degree of intercalation being very similar to that found in the SmC_d phase of compound **1¹²EO³OH**.

Table 3. Comparison of X-ray data and molecular dimensions of selected single chain compounds **1**.

Comp.	Phase	d/nm ($T/^\circ\text{C}$)	L/nm
1¹²(OH)₂	SmA _d	5.16 (169)	3.3
	SmC _d	5.05 (167)	3.3
1¹²EO³OH	SmC _d	5.57 (105)	3.7

XRD investigation of the Iso phases occurring immediately above the smectic-Iso phase transition of compounds **1¹²EO³(OH)₂** and **1¹²EO³OH**, shown in Fig. 4, indicates a higher intensity of the diffuse small angle scattering in the Iso phase of the glycerol derivative **1¹²EO³(OH)₂** compared to **1¹²EO³OH** having only one OH group. This indicates the formation of clusters in the Iso phase of **1¹²EO³(OH)₂** which is much weaker for compound **1¹²EO³OH** with only one terminal OH group. This could contribute to the observation that the enthalpy values of the Sm-Iso transition of the glycerol substituted compounds is only one half or even less than those measured for the related compounds with a single OH group (see Tables 1 and 2). It appears that for **1¹²EO³(OH)₂** significant cybotactic clusters are already formed in the Iso phase which then fuse to infinite layers at the Iso-Sm phase transition, whereas for **1¹²EO³OH** the clusters are much smaller and just at the Iso-Sm transition layer formation starts with much smaller clusters, thus leading to a larger enthalpy for the phase transition.

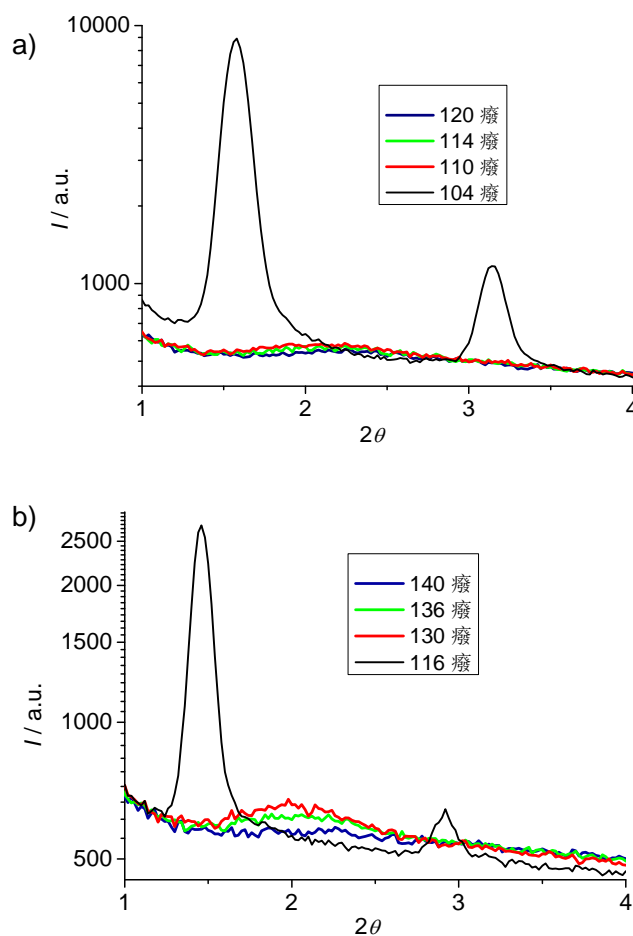
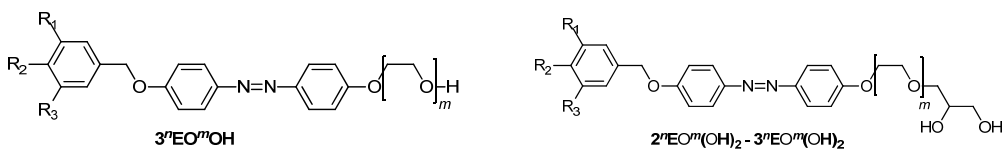


Figure 4. Small angle XRD patterns of compounds a) $1^{12}\text{EO}^3\text{OH}$ and b) $1^{12}\text{EO}^3(\text{OH})_2$ at the indicated temperatures in the smectic phase (black lines) and at different temperatures in the Iso phase in proximity to the SmA_d -Iso transition (colored lines), showing a significant cybotaxis for $1^{12}\text{EO}^3(\text{OH})_2$ being much weaker for $1^{12}\text{EO}^3\text{OH}$.

2.3 Thermotropic self-assembly of compounds 2 and 3 with two and three alkyl chains in columnar LC phases

Double and triple chain benzylether **2** and **3** are collated in Table 4. Except for compound $3^{14}\text{EO}^3\text{OH}$, other compounds show exclusively hexagonal columnar phases (Col_{hex}). In general the stability of LC phases increases with growing number of OH groups. The Col_{hex} -Iso transition enthalpies are in the range between $\Delta H = 0.4$ and 1.5 kJ mol^{-1} , which is about one order of magnitude smaller than those for the Sm-Iso transitions of compounds **1**, and there is obviously no dependence of the Col-Iso transition enthalpy on the number of OH groups.

Table 4. Mesophases, transition temperatures ($T/^\circ\text{C}$) and transitional enthalpy values ($\Delta H/\text{kJ mol}^{-1}$) of the multi chain compounds **2** and **3**^a



Comp	R ₁	R ₂ , R ₃	m	Phase transitions ($T/^\circ\text{C}$)	a/nm ($T/^\circ\text{C}$)	n _{cell}
2 ¹⁴ (OH) ₂	H	OC ₁₄ H ₂₉	0	Cr 115 [25.1] Col _{hex} 165 [1.5] Iso	6.65 (140)	13.0
3 ¹² (OH) ₂	OC ₁₂ H ₂₅	OC ₁₂ H ₂₅	0	Cr 59 [34.4] Col _{hex} 119 [0.7] Iso	6.20 (90)	9.6
3 ¹⁴ (OH) ₂	OC ₁₄ H ₂₉	OC ₁₄ H ₂₉	0	Cr 64 [36.7] Col _{hex} 115 [0.4] Iso		
3 ¹² EO ³ OH	OC ₁₂ H ₂₅	OC ₁₂ H ₂₅	3	Cr 74 [57.9] (Col _{hex} 70 [0.4]) Iso		
3 ¹⁴ EO ³ OH	OC ₁₄ H ₂₉	OC ₁₄ H ₂₉	3	Cr 78 [55.3] Iso ^b		
3 ¹² EO ³ (OH) ₂	OC ₁₂ H ₂₅	OC ₁₂ H ₂₅	3	Cr 66 [49.6] Col _{hex} 115 [0.9] Iso	7.17 (90)	11.3
3 ¹⁴ EO ³ (OH) ₂	OC ₁₄ H ₂₉	OC ₁₄ H ₂₉	3	Cr 71 [39.5] Col _{hex} 116 [0.5] Iso		

^a Abbreviations: Col_{hex} = hexagonal columnar phase with $p6mm$ symmetry; for conditions and other explanations see Table 1. ^b No LC phase was observed on cooling before crystallization at $T = 62^\circ\text{C}$:

There is a strong effect of the number of alkyl chains, reducing the mesophase stability with growing chain number (compare compounds **2**¹⁴(OH)₂ and **3**¹⁴(OH)₂ in Table 4). In contrast, the effects of the EO unit between azobenzene core and glycerol unit on melting temperatures and mesophase stability is only marginal (compare compounds **3**¹²EO³(OH)₂ and **3**¹²(OH)₂). The textures of the columnar mesophases, as observed between crossed polarizers, are characterized by ‘spherulitic’ domains (see Figs. 5a, S1a and c), combined with regions appearing completely dark, where the optic axis is normal to the LC film (homeotropic regions), see Figs. S1b. These textures indicate an optically uniaxial columnar LC phase. The orientation of the π -conjugated aromatic cores is deduced from the colour of the fans in the micrograph taken with a λ -retarder plate (Figs. 5b and S1c). The directions of yellow and blue fans with respect to the indicatrix of the retarder confirm the orientation of the high-index axis as radial to the fans. As the columns are tangential and the high-index axis is parallel to the π -conjugated aromatic cores. This means that in the columns the preferred direction of the intra-molecular π -conjugation pathway (i.e. the long axis of the azobenzene cores) is on average perpendicular to the column long axis, in line with the

proposed mode of self-assembly (see below).

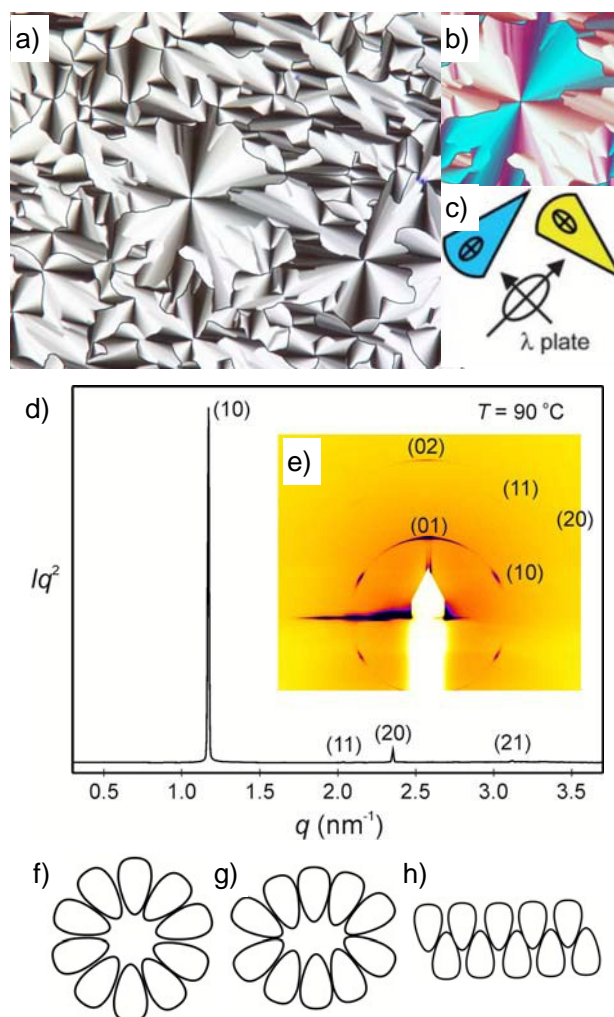


Figure 5. Investigation of compound $3^{12}(\text{OH})_2$ a) texture of the columnar phase at $T=90\text{ }^\circ\text{C}$ as observed between crossed polarizers; b) shows a section of the texture with additional λ -retarder plate and the orientation of the indicatrix of the λ -plate is shown in c); d) powder X-ray diffraction pattern at $T = 90\text{ }^\circ\text{C}$ and e) GISAXS pattern of a surface-aligned sample at $T = 90\text{ }^\circ\text{C}$; f-h) models showing the organization of the amphiphilic molecules, f) in circular columns, g) in elliptical columns and h) in ribbons; for more details, see Tables S4-7, Fig. S2.

The columnar phases of the double chain glycerol substituted compound $2^{14}(\text{OH})_2$, the three chain compound $3^{12}(\text{OH})_2$ and the related compound with additional $(\text{EO})_3$ unit $3^{12}\text{EO}^3(\text{OH})_2$ were investigated as representative examples by small-angle X-ray scattering (SAXS), and grazing-incidence small-angle X-ray scattering (GISAXS) on thin surface-aligned films on silicon using a synchrotron source (see Figs. 5d, e and S2). All columnar phases show three or four small angle reflections with a ratio of their reciprocal spacing $1 : 3^{1/2} : 2 : (7^{1/2})$ which can be indexed to the 10, 11, 20 (and 21) reflections of a

hexagonal lattice with $p6mm$ symmetry (Figs. 5d and S2c). The 2D pattern of an aligned sample of compound $\mathbf{3}^{12}(\text{OH})_2$ also confirms this phase assignment (Fig. 5e and S2b). Although SAXS was not carried out on all of the columnar phases, based on textural similarities (Fig. S1), it is very likely that the columnar phases of the other compounds represent the hexagonal columnar phases too. The number of molecules organized in a slice of the columns with a height of $h = 0.45$ nm (a typical value for the maximum of the diffuse wide angle scattering) n_{cell} was estimated using eq. (1) and assuming a density of $\rho = 1 \text{ g cm}^{-3}$ (N_A = Avogadro constant; M = molecular mass, see Table 4). The number decreases from $n_{\text{cell}} = 13$ for the two-chain compound $\mathbf{2}^{14}(\text{OH})_2$ to $n_{\text{cell}} = 10$ for the three-chain compound $\mathbf{3}^{12}(\text{OH})_2$. Introduction of the $(\text{EO})_3$ unit at constant alkyl chain volume leads to a slight increase of the number of molecules in the column cross section from $n_{\text{cell}} = 10$ to 11 for compound $\mathbf{3}^{12}\text{EO}^3(\text{OH})_2$.

$$n_{\text{cell}} = \left(\frac{a^2}{2}\right) \sqrt{3} h (N_A/M) \rho \quad (1)$$

These two- and triple-alkyl chain amphotropic azobenzene derivatives can be either considered as taper shaped molecules,^[40,41] providing a radial organization of the molecules in circular columnar aggregates, thus, directly leading to a packing of the circular columns on a hexagonal lattice (see model in Fig. 5f), or as polycatenar (three- and tetracatenar, respectively) mesogens, which can organize into ribbons of antiparallel organized molecules, resembling the organization in the smectic phases of the single chain compounds (model in Fig. 5h).^[42,43] In the latter case the time and space averaging of the ribbon local orientation would lead to the globally averaged hexagonal lattice. Probably the truth is somewhere in the middle, i.e. the columns have an elliptical shape which retains some ribbon-like organization in the middle and simultaneously the contact between polar groups and aliphatic chains in the periphery is minimized by fusing the aromatic regions to elliptical shells covering the polar regions (Fig. 5g). These elliptical columns are then arranged on a time and space averaged hexagonal lattice. This model is in line with the reconstructed electron density maps (see Fig. 6a, c) where the column centers with high electron density (purple) are surrounded by medium electron density shells (blue/green/yellow). The medium electron density shells might result from the rotational disorder of the elliptical columns leading to a space and time averaging of the high electron density polar cores and the low electron density alkyl chains in the continuum around the columns. In the column cores only the aromatic/polar cores of the elliptical columns

overlap on space and time average, leading to high electron density. Independent on the precise shape of the columns the rigid aromatics, the polar groups (polyether and glycerol unit) and the non-polar alkyl chains segregate into distinct domains. The polar units form the columns centers which are surrounded by the azobenzene cores and assembled on a hexagonal lattice within the lipophilic continuum mainly formed by the alkyl chains. The three alkyl chains of $\mathbf{3}^{12}(\text{OH})_2$ provide a stronger interface curvature leading to a 30 % decrease of the number of molecules organized in the cross section of the columns ($n_{\text{cell}} = 10$) compared to the double chain compound $\mathbf{2}^{14}(\text{OH})_2$ ($n_{\text{cell}} = 13$). Enlargement of the polar group by the $(\text{EO})_3$ chain increases the polar volume and this reduces the interface curvature, thus leading to a slight increase of the number of molecules organized in the cross section of the columns ($n_{\text{cell}} = 11$ for $\mathbf{3}^{12}\text{EO}^3(\text{OH})_2$).

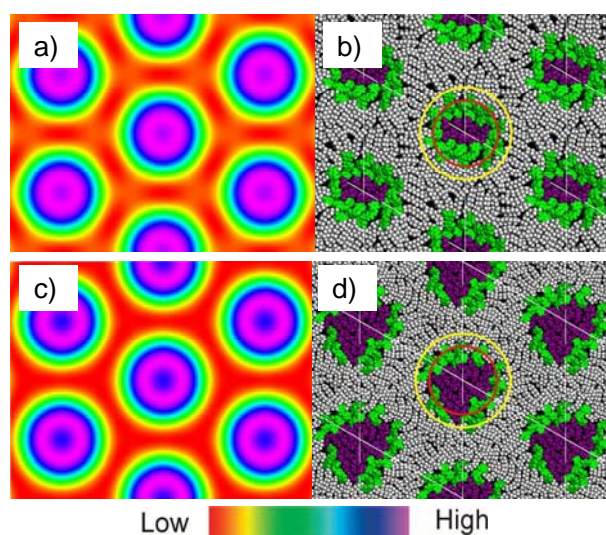


Figure 6. Electron density maps of the Col_{hex} phases of a) compound $\mathbf{3}^{12}(\text{OH})_2$ and c) compound $\mathbf{3}^{12}\text{EO}^4(\text{OH})_2$ as reconstructed from the synchrotron powder diffraction patterns (color code: purple/blue = high, green/yellow = medium and red = low electron density; for details of the reconstruction, see SI); b) snapshot of the structure of the Col_{hex} phase of $\mathbf{3}^{12}(\text{OH})_2$ and d) of $\mathbf{3}^{12}\text{EO}^3(\text{OH})_2$ after MD annealing (polar groups are colored purple and the aromatic cores green, alkyl chains gray); red and yellow circles represent the boundaries between high and medium and medium and low electron density regions in the electron density maps, respectively.

In Fig. 6 the reconstructed electron density maps of the Col_{hex} phases of compounds $\mathbf{3}^{12}(\text{OH})_2$ and $\mathbf{3}^{12}\text{EO}^3(\text{OH})_2$ (left) are compared with the molecular dynamics (MD) annealed models of the columnar phases (right). The MD annealed model of the columnar phase of $\mathbf{3}^{12}\text{EO}^3(\text{OH})_2$ (Fig. 6d) indicates that the polar chains form the majority of the column cores and the azobenzenes form a kind of shell separating the polar core from the aliphatic continuum, in which the alkyl chains are completely disordered and partly

interdigitated. The formation of a kind of aromatic shell is favored by the possibility of hydrogen bonding of the OH groups to the azo groups, to the electron rich aromatic π -systems and to the ether oxygens at the aromatics. The MD annealed model of the columnar phase of $3^{12}(\text{OH})_2$ (Fig. 6b) without EO units shows better defined shells of the aromatic cores with a larger degree of parallel alignment of the cores around the smaller core regions involving the polar groups (structure corresponding to model in Fig. 5g).

2.4 Effects of solvents and lyotropic self-assembly

The effect of protic solvents on the phase behavior of $1^{12}\text{EO}^3\text{OH}$ as representative example was investigated by POM and XRD. By adding ethylene glycol, the SmC phase of this compound is first stabilized, but already at $n_{\text{EO}} \sim 1$ ($n_{\text{EO}} = n(\text{EO})/n(1^{12}\text{EO}^3\text{OH})$) the stability of SmC phase decreases and a SmA phase occurs (Fig. 7). With further increase in solvent concentration, the SmC-SmA transition temperature decreases whereas the SmA phase stability rises. The SmC phase exhibits the typical schlieren texture as observed for the dry compound and the SmA phase shows oily streaks and homeotropic areas as characteristic of lyotropic SmA phases (Fig. 8). At $n_{\text{EO}} \sim 4$ the maximum of the phase stability is reached and with further growing solvent concentration the transition temperatures slightly decrease up to $n_{\text{EO}} \sim 11$ which represents the maximum uptake of solvent (Fig. 7). After reaching this concentration the system remained heterogeneous with excess solvent coexisting with the lyotropic LC system.

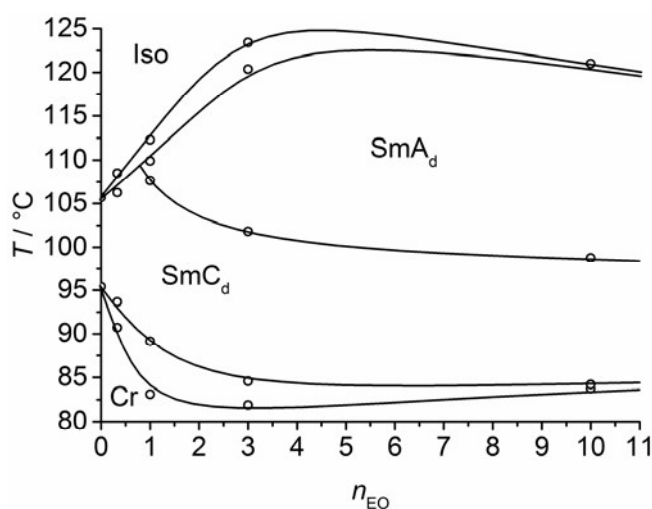


Figure 7. Phase diagram of the system $1^{12}\text{EO}^3\text{OH}$ /ethylene glycol (EO).

The system was in addition investigated by XRD for the concentrations $n_{\text{EO}} \sim 1$ (~ 10 wt% EO), $n_{\text{EO}} \sim$

3 (~ 30 wt% EO) and $n_{EO} \sim 10$ (~50 wt% EO). The XRD patterns showed the typical diffraction patterns of Smectic phases. There is a significant increase of the d -spacings with increasing solvent content, in line with a swelling of the polar layers by the added solvent molecules. Remarkably, the layer shrinkage at the SmA-SmC transition and in the temperature range of the SmC phase increases with increasing solvent content. In contrast, the layer spacing d remains nearly constant in the SmC phase region of the solvent-free sample (see Fig. 9). This could have different reasons, for example, the solvation of the head groups could change, i.e. the number of molecules separating the head groups laterally increases and simultaneously the number of solvent molecules arranged between the layers decreases with decreasing temperature. This could further lead to a stronger intercalation of the alkyl chains and an increase of the uniform (SmC) or average tilt (SmA) of the aromatic at lower temperature. The combined contribution of these effects is thought to lead to the observed effect.

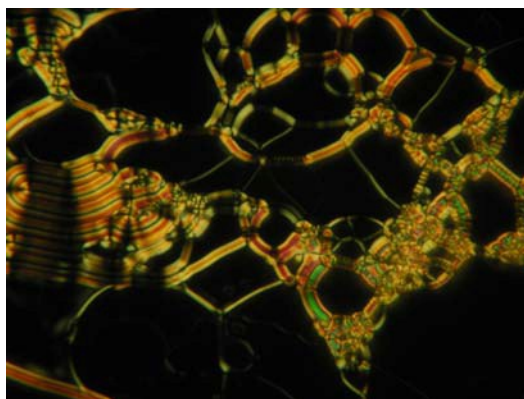


Figure 8. Texture of the solvent induced lyotropic SmA phase of $1^{12}EO^3OH$ at $T = 105$ °C in a mixture with ethylene glycol (EO) at $n_{EO} = 10$.

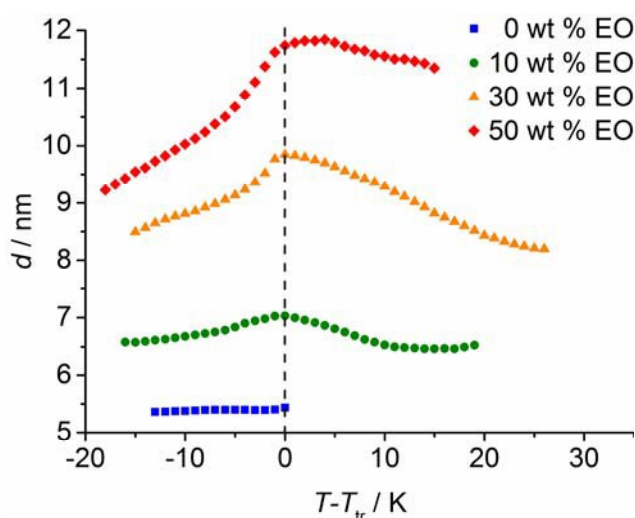


Figure 9. Temperature dependence of the layer spacing depending on the EO content of the system $1^{12}EO^3OH$ /ethylene glycol (EO).

A similar behaviour as with EO was also observed with water and formamide which were investigated by contact preparations. For this purpose the amphiphile and the solvent were placed side-by-side between two glass plates and the phases developing in the contact region due to the developing concentration gradient were observed under the polarizing microscope. In all cases a SmA phase was induced and an SmC-SmA-Iso phase sequence was found for the solvent enriched samples. For formamide a bit higher transition temperatures were observed for the solvent saturated sample (Cr 77 °C SmC 90 °C SmA 135 °C Iso), compared with EO, whereas for water the observed transition temperatures are lower (Cr 78 °C SmC 80 °C SmA 97 °C Iso for the water saturated sample). This is a bit surprising, as usually water provides the most efficient polar protic solvent, leading to the highest lyotropic phase stabilities.^[5]

Additional compounds were investigated with formamide as protic solvent. In the case of $1^{12}\text{EO}^3(\text{OH})_2$ with additional glycerol group there is an even stronger stabilization of the SmA phase, reaching about 180 °C for the formamide saturated sample. This formamide saturated sample crystallizes at 68 °C without formation of a SmC phase, i.e. there is a stronger destabilization of the tilted SmC phase. Compound $3^{12}(\text{OH})_2$ with a glycerol unit but without the EO segments behaves similar, the SmA phase being stabilized to > 200 °C, but the formamid saturated sample rapidly crystallizes already at 123 °C before the transition of the SmA to the SmC phase can take place.

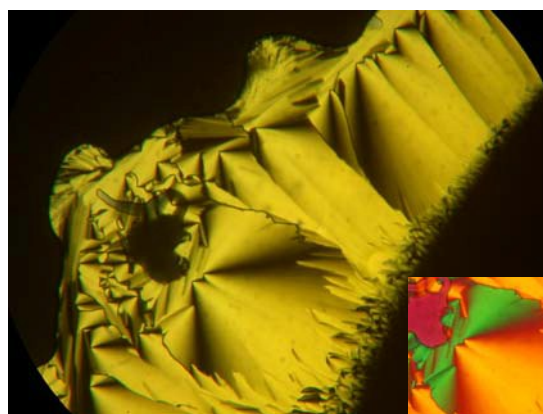


Figure 10. Texture of the solvent stabilized lyotropic Col_{hex} phase of $3^{12}\text{EO}^3(\text{OH})_2$ (right) at $T = 170^\circ\text{C}$ in the contact region with formamide (left) as observed on cooling, the inset shows the texture with additional λ -plate.

The lyotropic behavior of the three chain compounds is very different and for these compounds a strong dependence of the phase sequence on the type of polar group is observed. Compounds $3^{12}\text{EO}^3(\text{OH})_2$,

$3^{12}\text{EO}^3\text{OH}$ and $3^{12}(\text{OH})_2$ having identical alkyl chain lengths, but different types of polar groups were investigated as representative examples with formamide as polar protic solvent (contact preparations). The columnar phases of $3^{12}(\text{OH})_2$ and $3^{12}\text{EO}^3\text{OH}$, having either the glycerol group or the triethelenglycol chain, were completely removed in the contact region and only crystallization was observed at $T = 50\text{ }^\circ\text{C}$ for both compounds. In contrast, for compound $3^{12}\text{EO}^3(\text{OH})_2$, combining the EO chain with the glycerol group, a dramatic stabilization of the Col_{hex} phase was observed (see Fig. 10), it is retained up to the boiling point of this solvent at $210\text{ }^\circ\text{C}$. It appears that the molecular organization in columns with a polar interior restricts the effect of the solvent on the self assembly. In the case of relatively small polar groups the volume added by the solvent molecules to the polar groups distorts the formation of columnar aggregates, but it appears to be too small for a transition to a lamellar organization; therefore order is lost and an isotropic liquid is formed. For compound $3^{12}\text{EO}^3(\text{OH})_2$ with the largest polar group, involving a strong hydrogen bond donor group (the glycerol units) and having several additional hydrogen bonding acceptor sites along the EO chains, a small number of formamide molecules might be sufficient to dramatically increase the number of attractive hydrogen bondings, thus stabilizing the columnar aggregates without requiring too much additional space, and thus retaining the interface curvature. Moreover, as shown in Fig. 6d, the major part of the columns is formed by the polar groups, i.e. polar-apolar segregation is dominating the behaviour of $3^{12}\text{EO}^3(\text{OH})_2$. The azobenzenes, being strongly tilted and some of them organized nearly parallel to the column surface form a relatively thin shell. This might reduce the sensitivity to steric distortions of columnar self assembly and could lead to the very special behavior of this compound.

Investigation of aqueous systems was more difficult due to easy water evaporation, but in principle the behaviour can be considered as similar to formamide. So the Col_{hex} phase of $3^{12}\text{EO}^3(\text{OH})_2$ is retained in the contact region in the whole temperature region available for investigation, whereas for $3^{12}\text{EO}^3\text{OH}$ and $3^{12}(\text{OH})_2$ the columnar phases are removed for the water saturated samples. It appears that for $3^{12}(\text{OH})_2$ an additional lamellar phase is induced in the water saturated sample with a clearing temperature of $71\text{ }^\circ\text{C}$, but this is not completely sure due to the above mentioned difficulties in handling these amphiphile water systems.

2.5 Photoisomerization behavior

All compounds **1-3** exhibit the expected reversible photoresponsive behavior (see Fig. 11). All azobenzene derivatives in the *E*-form show a strongly absorption band in the UV region (~ 360 nm) which is attributed to the $\pi\text{-}\pi^*$ transition, and a weakly absorbing band in the visible region (~ 450 nm) due to the $n\text{-}\pi^*$ transition. The *E*-form is generally more stable than the *Z*-form, but each isomer can be converted into the other by light-irradiation caused a decrease of the absorption at around 355 nm and an increase at around 450 nm. For example, dark incubations of a dichloromethane solution (1×10^{-5} M) of **1¹²EO³OH** have a maximum absorbance at 358 nm corresponding to the *trans*-azobenzene chromophore ($\pi\text{-}\pi^*$ transition). Irradiation of this solution with 365 nm light resulted in the photoisomerization from *trans*-azobenzene to *cis*-azobenzene chromophore, as evidenced by a decrease in absorbance at 358 nm and an increase at around 450 nm ($n\text{-}\pi^*$ transition). Also the absorbance at 313 nm ($\pi\text{-}\pi^*$ transition) increased. The *E-Z* transition was completely achieved in 35s (see Fig. 11a). Under visible light, the reverse *E-Z* transition process was achieved within 6 min (see Fig. 11b).

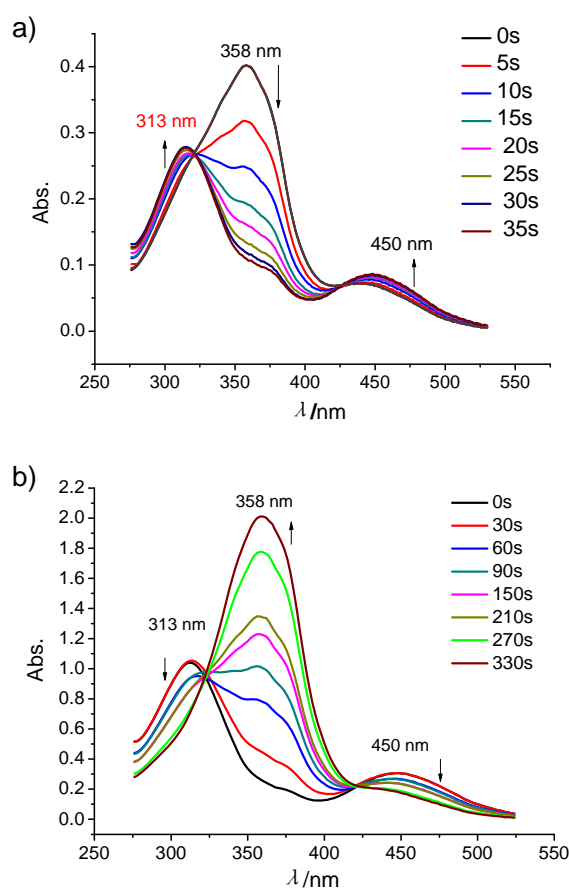


Figure 11. UV Spectra of **1¹²EO³OH** in CH_2Cl_2 solution ($c = 10^{-5}$ mol L^{-1}), changing with the time: a) from *trans*- to *cis*-azobenzene under irradiation with 365 nm light; b) from *cis*- to *trans*-azobenzene under irradiation with visible light; for additional examples, see Figs S3, S4.

The effect of *E*-to-*Z* photo-isomerization caused by the UV irradiation on the thermotropic LC phases was investigated with compound **1¹²EO³OH** as an example. The sample was placed between two thin quartz glass plates to form a thin film and placed on a Linkam hot stage that can control the sample temperature within 0.1 °C. The sample was cooled from the isotropic liquid state to 98 °C in the range of the SmC_d phase (see Fig. S6a). After annealing for 5 minutes the sample was exposed to UV irradiation at 365 nm (5 mW cm⁻²) for 60 s. After ~20 s exposure time the Schlieren texture of the SmC_d phase has changed to a plain fan texture separated by homeotropic areas, indicating that the SmC_d phase is replaced by a SmA phase (most probably SmA_d; see Fig. S6b, c). After thermal annealing at the same temperature of 98 °C without irradiation a slow change of the texture back to the SmC_d phase took place, indicating a thermal *Z*-*E* isomerization (see Fig. S6d, e). So the *E*-*Z* photo-isomerization allows a reversible switching between SmC and SmA at a fixed temperature. This is due to a change of the phase transition temperatures. For example, a sample exposed for 30 s has the phase sequence Cr 86 °C SmC 94 °C SmA 99 °C Iso. This means that photoisomerization induces a SmA phase and reduces the Sm-Iso transition temperature (compare with Table 1). It appears that the isomerization process in the LC state is significantly slower than in isotropic solution. Nevertheless, in the LC state the photoinduced *E*-to-*Z* transitions is still sufficiently fast and requires only a few seconds to induce a SmA phase, whereas the thermal relaxation to the SmC phases is much slower, requiring about 1 hour at the used temperature. Such photoisomerizations could be useful for light sensitive displays or for data storage applications.

3. Conclusion

A series of amphotropic azobenzene derivatives with different number of alkyl chains and distinct structure of the polar groups was synthesized and investigated with respect to thermotropic and lyotropic self-assembly in LC phases. Most compounds with only one *n*-alkyl chain form fluid tilted smectic phases with double layer structure (SmC_d). Compounds with a single hydroxyl group form exclusively the SmC_d phase whereas a SmC_d/SmA_d dimorphism was observed for most of the related diols. SmA phases were induced and stabilized by addition of protic solvents. This means that increased head group size favors SmA phases, but nevertheless broad regions of lyotropic SmC phases were retained. Such SmC phases are rarely observed in lyotropic LC phases and these materials are of interest as lyotropic ferroelectrics after introduction of chirality.^[10b] The SmC-SmA transition can be considered as mainly resulting from the

randomization of the tilt by the lateral separation of the molecules by the solvent molecules located around the polar groups. The increased effective polar group volume also reduces the tilt correlation between the layers.

Compounds with two or three alkyl chains form exclusively Col_{hex} phases and there is a strong effect of protic solvents, stabilizing Col_{hex} phases of compounds combining EO chains with glycerol units and removing columnar phases for compounds having only one of them, either EO chains or glycerol units. All amphiphiles show photo responsive behavior which makes these compounds interesting for potential applications as photo responsive amphiphiles and LC.

Acknowledgements Support by the National Natural Science Foundation of China [No. 21364017, No. 21274119, No. 21374086], the Yunnan Natural Science Foundation (2013FA007), DFG FOR 1145 (Ts 39/21-2), MP acknowledges the support by the Cluster of Excellence “Nanostructured Materials” of the government of Saxony-Anhalt, JRB acknowledges financial support by the “Landesgraduiertenförderung” of the state Baden-Württemberg.

References

-
- [1] J. W. Steed, J. L. Atwood, *Encyclopedia of Supramolecular Chemistry*, Marcel Dekker, New York, 2004; J. M. Lehn, *Supramolecular Chemistry*, VCH, Weinheim, 1995.
- [2] a) C. Tschierske, *Angew. Chem. Int. Ed.*, 2013, **52**, 8828–8878; b) B. Donnio, D. Guillon, *Adv. Polym. Sci.*, 2006, **201**, 145–155; c) T. Kato, N. Mizoshita, K. Kishimoto, *Angew. Chem.*, 2006, **118**, 44–74; d) M. Lee, B.-K. Cho, W.-C. Zin, *Chem. Rev.*, 2001, **101**, 3869–3892; e) I. M. Saez, J. W. Goodby, *J. Mater. Chem.*, 2005, **15**, 26–40; f) G. Ungar, X. Zeng, *Soft Matter.*, 2005, **1**, 95–106.
- [3] H. Ringsdorf, B. Schlarb and J. Venzmer, *Angew Chem.*, 1988, **100**, 117–162.
- [4] a) R. Duran and P. Gramain, *Makromol Chem.*, 1987, **188**, 2001–2009; b) R. Duran, D. Guillon, P. Gramain and A. Skoulios, *J. Phys (Paris).*, 1988, **49**, 1455–1466; c) H. R. Allcock and C. Kim, *Macromolecules.*, 1989, **22**, 2596–2602; d) V. Percec and C. -S. Hsu, *Polym Bull.* **1990**, 23, 463–470; e) V. Percec, D. Tomazos, J. Heck, H. Blackwell and G. Ungar, *J. Chem. Soc. Perkin Trans.*, 1994, 2, 31–44.

- [5] a) C. Tschierske, *Prog. Polym. Sci.*, 1996, **21**, 775–852; b) M. Kölbel, T. Beyersdorff, C. Tschierske, S. Diele, J. Kain, *Chem. Eur. J.*, 2000, **6**, 3821–3837; c) C. Tschierske, *Curr Opin Colloid Interf. Sci.*, 2002, **7**, 355–370.
- [6] a) B. Neumann, C. Sauer, S. Diele, C. Tschierske, *J. Mater. Chem.*, 1996, **6**, 1087–1098; b) C. Tschierske, J. A. Schröter, N. Lindner, C. Sauer, S. Diele, R. Festag, M. Wittenberg, J.-H. Wendorff, *SPIE.*, 1998, **3319**, 8–13; c) C. Sauer, S. Diele, C. Tschierske, *Liq. Cryst.*, 1997, **23**, 911–917; d) C. Sauer, S. Diele, N. Lindner, C. Tschierske, *Liq. Cryst.*, 1998, **25**, 109–116.
- [7] N. Lindner, M. Kölbel, C. Sauer, S. Diele, J. Jokiranta, C. Tschierske, *J. Phys. Chem., B*, 1998, **102**, 5261–5273.
- [8] A. Bubnov, M. Kašpar, V. Hamplová, U. Dawin and F. Giesselmann, *J. Org. Chem.*, 2013, **9**, 425–436.
- [9] N. Pietschmann, A. Lunow, G. Brezesinski, C. Tschierske, F. Kuschel, H. Zschke, *Colloid and Polymer Science.*, 1991, **269**, 636–639.
- [10] a) J. R. Bruckner, D. Krueerke, J. H. Porada, S. Jagiella, D. Blunk and F. Giesselmann, *J. Mater. Chem.*, 2012, **22**, 18198–18203; b) J. R. Bruckner, J. H. Porada, C. F. Dietrich, I. Dierking, and F. Giesselmann, *Angew. Chem. Int. Ed.*, 2013, **52**, 8934–8937.
- [11] a) C. Tschierske, A. Lunow, D. Joachimi, F. Hentrich, D. Girdziunaite, H. Zschke, A. Mädicke, G. Brezesinski, F. Kuschel, *Liq. Cryst.*, 1991, **9**, 821–829; b) H. Müller, C. Tschierske, *J. Chem. Soc. Chem. Commun.*, 1995, 645–646.
- [12] a) D. Joachimi, C. Tschierske, A. Öhlmann, W. Rettig, *J. Mater. Chem.*, 1994, **4**, 1021–1027; b) D. Joachimi, A. Öhlmann, W. Rettig, C. Tschierske, *J. Chem. Soc. Perkin Trans.*, 1994, **2**, 2011–2019.
- [13] T. Kato, *Angew. Chem. Int. Ed.*, 2010, **49**, 7847–7848.
- [14] a) T. Ube and T. Ikeda, *Angew. Chem. Int. Ed.*, 2014, **53**, 10290–10299; b) H. M. Dhammika Bandarab and S. C. Burdette, *Chem. Soc. Rev.*, 2012, **41**, 1809–1825.
- [15] a) T. Ikeda, J. Mamiya, Y. Yu, *Angew. Chem. Int. Ed.*, 2007, **46**, 506–528; b) E. V. Fleischmann, R. Zentel, *Angew. Chem. Int. Ed.*, 2013, **52**, 8810–8827; *Angew. Chem.*, 2013, **125**, 8972–8991.
- [16] a) Y. Yu, M. Nakano, T. Ikeda, *Nature.*, 2003, **425**, 145–145; b) Y. Yu, M. Nakano, A. Shishido, T. Shishido, T. Ikeda, *Chem. Mater.*, 2004, **16**, 1637–1643; c) M. Kondo, Y. Yu, T. Ikeda, *Angew. Chem., Int. Ed.*, 2006, **45**, 1378–1382; d) Y. Yu, T. Maeda, J. Mamiya, T. Ikeda, *Angew. Chem. Int. Ed.*, 2007, **46**, 881–883; e) Y. Zhang, J. Xu, F. Cheng, R. Yin, C. -C. Yen, Y. Yu, *J. Mater. Chem.*, **2010**, **20**, 7123–7130.
- [17] a) R. F. Tabor, D. D. Tan, S. S. Han, S. A. Young, Z. L. E. Seeger, M. J. Pottage, C. J. Garvey, and B. L. Wilkinson, *Chem. Eur. J.*, 2014, **20**, 13881–13884.
- [18] X. M. Liu, B. Yang, Y. L. Wang, J. W. Wang, *Chem. Mater.*, 2005, **17**, 2792–2799.
- [19] a) S. K. M. Nalluri, B. Jan Ravoo, *Angew. Chem. Int. Ed.*, 2010, **49**, 5371–5374; *Angew. Chem.*, 2010, **122**, 5499–5502; b) F. P. Hubbard, G. Santonicola, E. W. Kaler, N. L. Abbott, *Langmuir.*, 2005, **21**, 6131–6136.
- [20] C. T. Jr. Lee, K. A. Smith, T. A. Hatton, *Macromolecules.*, 2004, **37**, 5397–5405.

- [21] J. Eastoe and A. Vesperinas, *Soft Matter.*, 2005, **1**, 338–347.
- [22] a) N. Drillaud, E. Banaszak-Leonard, I. Pezron, C. Len, *J. Org. Chem.*, 2012, **77**, 9553–9561; b) R. Bianchini, G. Catelani, R. Cecconi, F. D'Andrea, E. Frino, J. Isaad, M. Rolla, *Carbohydr. Res.*, 2008, **343**, 2067–2074.
- [23] a) J. M. Kuiper and J. B. F. N. Engberts, *Langmuir.*, 2004, **20**, 1152–1160; b) Y. Okuia and M. HanRational, *Chem. Commun.*, 2012, **48**, 11763–11765; c) E. Chevallier, C. Monteux, F. Lequeux, and C. Tribet, *Langmuir.*, 2012, **28**, 2308–2312.
- [24] a) T. G. Shang, K. A. Smith, and T. A. Hatton, *Adv. Mater.*, 2014, **26**, 1918–1922; b) S. Aya, H. Obara, D. Pocięcha, F. Araoka, K. Okano, K. Ishikawa, E. Gorecka, T. Yamashita, and H. Takezoe, *Adv. Mater.*, 2014, **26**, 1918–1922; c) M. Badis, M. H. Guermouche, J. -P. Bayle, M. Rogalski, and E. Rogalska, *Langmuir.*, 2004, **20**, 7991–7997.
- [25] C. Kördel, C. S. Popeney and R. Haag, *Chem. Commun.*, 2011, **47**, 6584–6586.
- [26] Y. Y. Lin, Y. Qiao, C. Gao, P. F. Tang, Y. Liu, Z. B. Li, Y. Yan, and J. B. Huang, *Chem. Mater.*, 2010, **22**, 6711–6717.
- [27] a) D. G. Whitten, L. H. Chen, H. C. Geiger, J. Perlstein, and X. D. Song, *J. Phys. Chem. B.*, 1998, **102**, 10098–10111; b) E. H. G. Backus, J. M. Kuiper, J. B. F. N. Engberts, B. Poolman, and M. Bonn, *J. Phys. Chem. B.*, 2011, **115**, 2294–2302.
- [28] a) D. -Y. Kim, S.-A. Lee, Y. -J. Choi, S. -H. Hwang, S. -W. Kuo, C. Nah, M. -H. Lee, and K. -U. Jeong, *Chem. Eur. J.*, 2014, **20**, 5689–5695; b) Z. H. Shi, D. Z. Chen, H. J. Lu, B. Wu, J. Ma, R. S. Cheng, J. L. Fang and X. F. Chen, *Soft Matter.*, 2012, **8**, 6174–6184.
- [29] N. Laurent, N. Lafont, F. Dumoulin, P. Boullanger, G. Mackenzie, P. H. J. Kouwer, J. W. Goodby, *J. Am. Chem. Soc.*, 2003, **125**, 15499–15506.
- [30] B. Soberats, E. Uchida, M. Yoshio, J. Kagimoto, H. Ohno and T. Kato, *J. Am. Chem. Soc.*, 2014, **136**, 9552–9555.
- [31] F. A. Khan, K. Parasuraman, B. Donnio, *Tetrahedron.*, 2010, **66**, 8745–8755.
- [32] a) R. Willstätter, M. Benz, *M. Chem. Ber.*, 1906, **39**, 3492–3503; b) W. H. Wei, T. Tomohiro, M. Kodaka, and H. Okuno, *J. Org. Chem.*, 2000, **65**, 8979–8987.
- [33] V. Van Rheenen, D. Y. Cha, W. M. Hartley, *Org. Synth.*, 1978, **58**, 43–51.
- [34] T. P. Rieker, N. A. Clark, G. S. Smith, D. S. Parmar, E. B. Sirota, C. R. Safinya, *Phys. Rev. Lett.*, 1987, **59**, 2658–2661.
- [35] Y. Ouchi, H. Takano, H. Takezoe, A. Fukuda, *Jpn. J. Appl. Phys.*, 1988, **27**, 1–7.
- [36] N. A. Clark, T. P. Rieker, J. E. McLennan, *Ferroelectrics.*, 1988, **85**, 79–97.
- [37] G. W. Gray, J. W. Goodby, *Smectic Liquid Crystals – Textures and structures*, Leonard Hill, sgoe and London, 1984.
- [38] CAChe 3.2, Oxford Molecular Ltd. Oxford, UK, 1999.
- [39] Identical values were obtained with CPK models.
- [40] K. Borisch, S. Diele, P. Göring, H. Kresse, C. Tschierske, *J. Mater. Chem.*, 1998, **8**, 529–543.

-
- [41] B. M. Rosen, C. J. Wilson, D. A. Wilson, M. Peterca, M. R. Imam, V. Percec, *Chem. Rev.*, 2009, **109**, 6275 – 6540.
- [42] a) H. -T. Nguyen, C. Destrade, J. Malthete, *Adv. Mater.*, 1997, **9**, 375-388; b) M. Gharbia, A. Gharbi, H. T. Nguyen, J. Malthete, *Curr. Opin Coll Interf. Sci.*, 2002, **7**, 312-325.
- [43] N. G. Nagaveni, M. Gupta, A. Roy and V. Prasad, *J. Mater. Chem.*, 2010, **20**, 9089–9099.

Graphical Abstract

Amphotropic azobenzene derivatives with oligooxyethylene and glycerol based polar groups

Xiaoping Tan,^{‡a} Ruilin Zhang,^{‡ab} Chunxiang Guo,^a Hongfei Gao,^a Xiaohong Cheng,^{*a} Feng Liu,^{*c} Johanna R. Bruckner,^d Frank Giesselmann,^{*d} Marko Prehm,^e Carsten Tschierske^{*c}

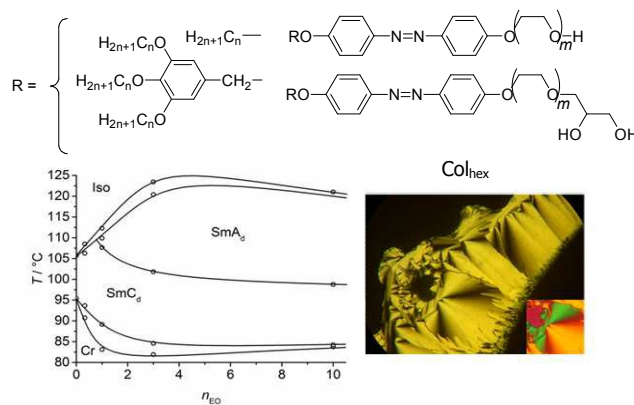
^a Key Laboratory of Medicinal Chemistry for Natural Resources, Yunnan University, Kunming 650091, P. R. China

^b Forensic Medicine of Kunming Medical University, Kunming 650500, P. R. China

^c State Key Laboratory for Mechanical Behavior of Materials, Xi'an Jiaotong University, Xi'an, 710049, P. R. China

^d University of Stuttgart, Institute of Physical Chemistry, Pfaffenwaldring 55, D-075069 Stuttgart, Germany

^e Martin Luther University Halle-Wittenberg, Institute of Chemistry, Kurt-Mothes Str. 2, 06120 Halle/Saale, Germany



Amphiphilic azobenzenes with one to three lipophilic alkyl chains and a nonionic polar group based on oligoethylene glycol (EO) and racemic 3-glyceryl units self assemble into double layer smectic and hexagonal columnar liquid crystalline phases, which are strongly affected and modified by protic solvents.